

## Buried Objects Segmentation and Detection in GPR B Scan Images

**Gozde ALTIN**  
Kocaeli University

**Arif DOLMA**  
Kocaeli University

**Abstract:** Identification of buried objects through Ground Penetrating Radar B scan (GPR-B) images needs high computational techniques and long processing time due to curve fitting or pattern recognition methods. In this study, an efficient and fast recognition system is proposed for detection of buried objects region. Previously, GPR-B scan images of objects with different shapes in various depths were obtained by using gprMax simulation program. The detection process is categorized into four steps. The GPR-B images are transformed at first step. Then, they are thresholded to obtain potential buried object regions. Third step of the system is hough transform in order to eliminate ground surface. Finally, an estimated region analysis is performed. The results show high performance with fully automatic segmentation. The processing time for detection of buried object is in the range of 1.234 - 2.232 seconds. It can be observed that this technique is faster than other studies in the literature. Consequently, it may be used in real time applications for GPR devices.

**Keywords:** Ground penetrating radar, GprMax, image processing, Otsu thresholding, Hough transform

### Introduction

The non-destructive techniques to explore underground materials have recently had great interest by public. Especially, private entities have applied it on widespread areas such as gas exploration, pipe localization, geology and archaeology etc. It is necessary to use an appropriate sensor for underground imaging in accordance with types of applications. Ground Penetrating Radar (GPR) has been widespread for subsurface mapping via using electromagnetic waves with high frequency [1]. GPR can scan in the range from various centimeters to a few meters because it operates on the principle of transmitting and receiving electromagnetic waves. There are several studies for automatic detection of buried objects from GPR images. Capineri et al. suggested hough transform to describe the ground plane in GPR image [2]. Brunzell could separate the reflected signal from soil surface and underground objects by means of appropriate algorithms and classical detection methods [3]. Delbo et al. used wavelet transform to reduce noise on GPR images and on top that hyperbolic identification is provided via fuzzy clustering algorithms [4]. With some preprocessing algorithms, hyperbolic structures in the GPR image are foregrounded and automatically classified with artificial neural networks by Gamba et al. [5]. Noise reduction on GPR image is provided by preprocessing algorithms and then artificial neural network segmented them. Hyperbolic lines are identified using hough transform [6]. Youn et al. examined the effects of different levels of clutter and noises on performance of artificial neural networks in GPR images [7]. Rossini detected underground objects by using wavelet transform and mathematical interpolation model [8]. Shihab et al. computed higher order statistical features for neural network classification in order to distinguish between soil ground and underground objects [9]. Gamba et al. obtained high performance for detection of buried objects by combination of artificial neural network and template matching algorithms [10]. Falorni et al. used monodimensional gradient filter to identify hyperbolic patterns [11]. Dell'Acqua et al. presented an approach based on 3-D Radon transform to eliminate interference and masking in GPR images [12]. Ting-Jun extracted hyperbola apexes by using peak tracing and hyperbola symmetry [13].

The aim of this paper is to offer an efficient and fast fully automatic image processing method for detection of buried objects in GPR images. The attractive feature of this method is able to analyze GPR images without the

---

- This is an Open Access article distributed under the terms of the Creative Commons Attribution-Noncommercial 4.0 Unported License, permitting all non-commercial use, distribution, and reproduction in any medium, provided the original work is properly cited.

- Selection and peer-review under responsibility of the Organizing Committee of the Conference

need of any specialist support. The proposed system includes preprocessing, segmentation, object detection stages. The preprocessing process for GPR images require to separate different RGB color space. Red channel of GPR images is the most appropriate platform for the image segmentation. Then, the images are segmented by Otsu thresholding method. The hyperbolas is identified by hough transform. Finally, the region analysis is implemented. The rest part of the paper is organized as follows. It is introduced that how to obtain GPR signals and images in Section II. The proposed image processing algorithm is described in Section III. The experimental results drawn in Sections IV. Section V inserts the conclusion part.

## Materials

Python is used for design of gprMax program which has not any user interface. It is open source program based on simulation of electromagnetic wave propagation. It tries the Finite Difference Time Domain (FDTD) method in order to solve Maxwell equations in three dimension. GPR data can be obtained by gprMax program. GPR data can be obtained in three ways: A-scan, B-scan and C-scan.

The data is taken by an unique transceiver antenna at a fixed position (x, y) as shown in Figure 1 for GPR A scan signal. The propagation duration of the electromagnetic wave varies depending on its speed. A scan signals can be used to detect locations of buried objects via propagation duration.

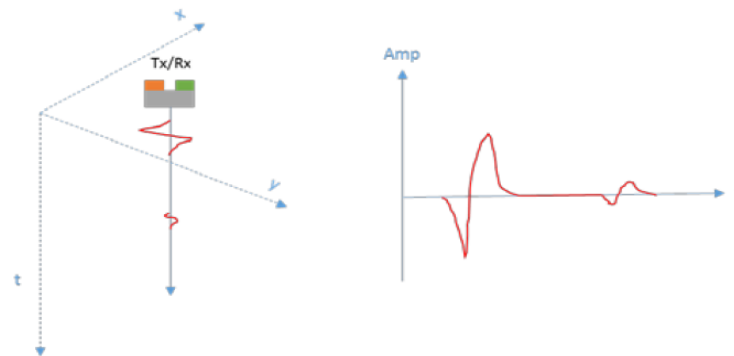


Figure 1. Example of GPR A Scan Signal

GPR B scan images consist of A scan signals along the x axis measured at regular intervals as shown in Figure 2. A GPR image is generated in accordance with the characteristic of the received signal. The vertical axis (y) represents the depth of the ground in relation to the signal time (t), while the horizontal axis (x) symbolizes the surface distance. Buried objects in B scan image are displayed as hyperbola.

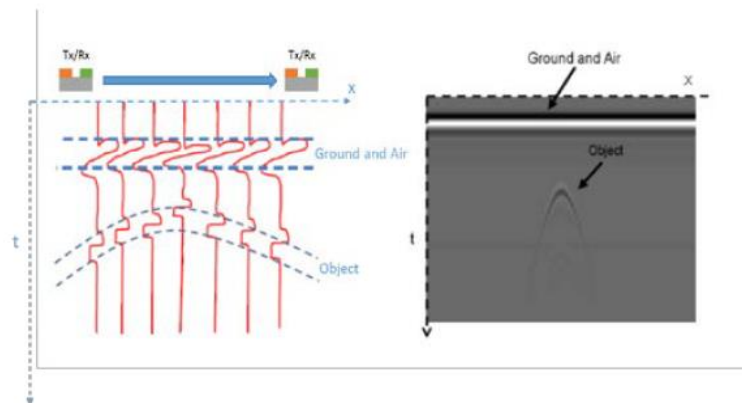


Figure 2. Example of GPR B Scan Image

GPR C scan is three-dimensional image which is generated by combining simultaneous B scan images on the xy plane. Signal time (t) represents depth of the ground. Particularly, y axis is important role for construction GPR C scan which is not preferred over other scan types because it is too expensive and taking much more time.

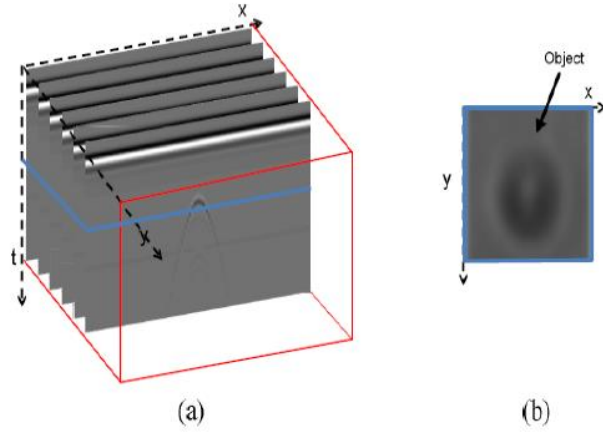


Figure 3. a) C-scan Measurement b) C scan image

## Methods

### RGB Color Space

The basic three colors are Red (R), Green (G) and Blue (B) which are mixed to get any color in digital color image. The RGB color space can be transformed into a 3D color space with coordinate axes red, green, and blue. In grayscale digital images, the pixels contain all the intensity information starting from the weakest to the strongest. A colored image is converted to a grayscale, which makes it easier to perceive desired regions for image segmentation. The R, G, B pixel values in the color images are converted to gray values as shown in Eq. 1. Also, Y represents gray level of color image.

$$Y = 0.2989R + 0.587G + 0.114B \quad (1)$$

### Otsu Thresholding

Otsu thresholding method is applied on the Red channel of GPR B scan images. Gray scale distribution histogram and average gray pixel value are used in the most of threshold segmentation method. The pixels are divided into two classes as  $C_0$  and  $C_1$  at gray level  $t$ .  $C_0$  is in the range from 0 to  $t-1$  and  $C_1$  is between  $t$  and  $L-1$ . Gray level probability distributions are calculated for  $C_0$  and  $C_1$  as in Eq.2 and Eq.3.

$$\omega_0 = P(C_0) = \sum_{i=0}^{t-1} P_i \quad (2)$$

$$\omega_1 = P(C_1) = \sum_{i=t}^{L-1} P_i \quad (3)$$

The means of  $C_0$  and  $C_1$  classes are computed as in Eq.4 and Eq.5.

$$\mu_0 = \sum_{i=0}^{t-1} i.P_i / \omega_0 \quad (4)$$

$$\mu_1 = \sum_{i=t}^{L-1} i.P_i / \omega_1 \quad (5)$$

The total mean of  $C_0$  and  $C_1$  classes is denoted by Eq.6.

$$\mu_T = \omega_0\mu_0 + \omega_1\mu_1 \quad (6)$$

The variances of  $C_0$  and  $C_1$  classes are

$$\sigma_0^2 = \sum_{i=0}^{l-1} (i - \mu_0)^2 p_i / \omega_0 \quad (7)$$

$$\sigma_1^2 = \sum_{i=l}^{k-1} (i - \mu_1)^2 p_i / \omega_1 \quad (8)$$

The within-class variance is computed as in Eq. 9.

$$\sigma_w^2 = \sum_{k=0}^M \omega_k \sigma_k^2 \quad (9)$$

The between-class variance is formulated as Eq. 10.

$$\sigma_b^2 = (\omega_0)(\mu_0 - \mu_T)^2 + (\omega_1)(\mu_1 - \mu_T)^2 \quad (10)$$

The total gray variance is

$$\sigma_T^2 = \sigma_w^2 + \sigma_b^2 \quad (11)$$

In Otsu method, the within-class variance is maximized and the between-class variance is minimized by threshold value  $t$ .

### Hough Transform and Region Analysis

The Hough transform can be defined as a transformation of a point to a parameter space of  $x, y$  plane. The parameter space is occurred in accordance with the shape of interest objects. A straight line passing through the  $x_1, x_2$  point on the  $x, y$  plane is expressed as shown in Eq. 12.

$$y_1 = ax_1 + b \quad (12)$$

In this notation, which expresses an equation of a straight line in the Cartesian coordinate system, it represents the parameters  $a$  and  $b$ . This equation is not used in the Hough transformation for straight line description. Because the lines perpendicular to the  $x$  axis have infinite value. This requires that the parameter space of  $a$  and  $b$  be in infinite size. Therefore,  $\theta$  and  $p$  are used for representation of a straight line. Line equation in parameter space is given in Eq. 13.

$$p = x \cos(\theta) - y \sin(\theta) \quad (13)$$

Circles can be expressed more simply in parameter space than line representation. Because the parameters of the domain can be transferred directly to the parameter space as in Eq. 14.

$$r^2 = (x-a)^2 + (y-b)^2 \quad (14)$$

There are three parameters of the circle as  $a, b$  and  $r$  which denote direction and radius of circle, respectively. The parametric representation of the circle is as in Eq. 15 and Eq. 16.

$$x = a + r \cos(\theta) \quad (15)$$

$$y = b + r \sin(\theta) \quad (16)$$

The parametric space of the circle belongs to  $R_3$ ; on the other hand, the parametric space of line belongs to  $R_2$ . As the parameters representing the shape increase, the parameter space  $R$  will also increase and the Hough transformation will become more complex.  $a, b$ , and  $r$  are the parameters to be used for the circular Hough transformation. The circles that can be drawn are centered at any point on the  $ab$  plane. When  $r$  is radius of the

circle, this circle can be plotted on the parameter space. Region analysis bases on regionalization and hyperbolic identification. One or more connected pixel region can be combined in a single region. Regionalization starts by evaluating each pixel. If a pixel is found, the other pixels in the same region are checked in the algorithm loop. It is ensured that the hyperbolas regions are drawn by taking the eccentricities and their areas into consideration after all regions are obtained.

### Proposed Method

In GPR B scan images, many different methods have been proposed for extracting the ground plane and plotting the estimated location of the buried objects. Within the scope of this study, working in RGB color space is suitable platform for segmenting of the ground plane and the location of the buried objects. For this reason, red channel is selected in RGB space and soil and objects are segmented by using the Otsu threshold method. Soil planes are extracted by Hough transformation. Estimated buried object region is drawn by region analysis method.

### Results and Discussion

Implementation results and performance results of proposed algorithms are described in this section. The algorithm is applied on 8 pieces GPR B scan images which are produced by gprMax program based on python software. All images are resized as 2629x1441 pixel. It is performed in a computer with Aspire 5930 Intel Core 2 Duo P8600 2.0 GHz Montevina processors. 2GB of RAM with 256 MB of GDDR3 GeForce supported system memory with nVIDIA 9600M GT graphics card is used. The image processing results of the algorithm are described in Figure 4.

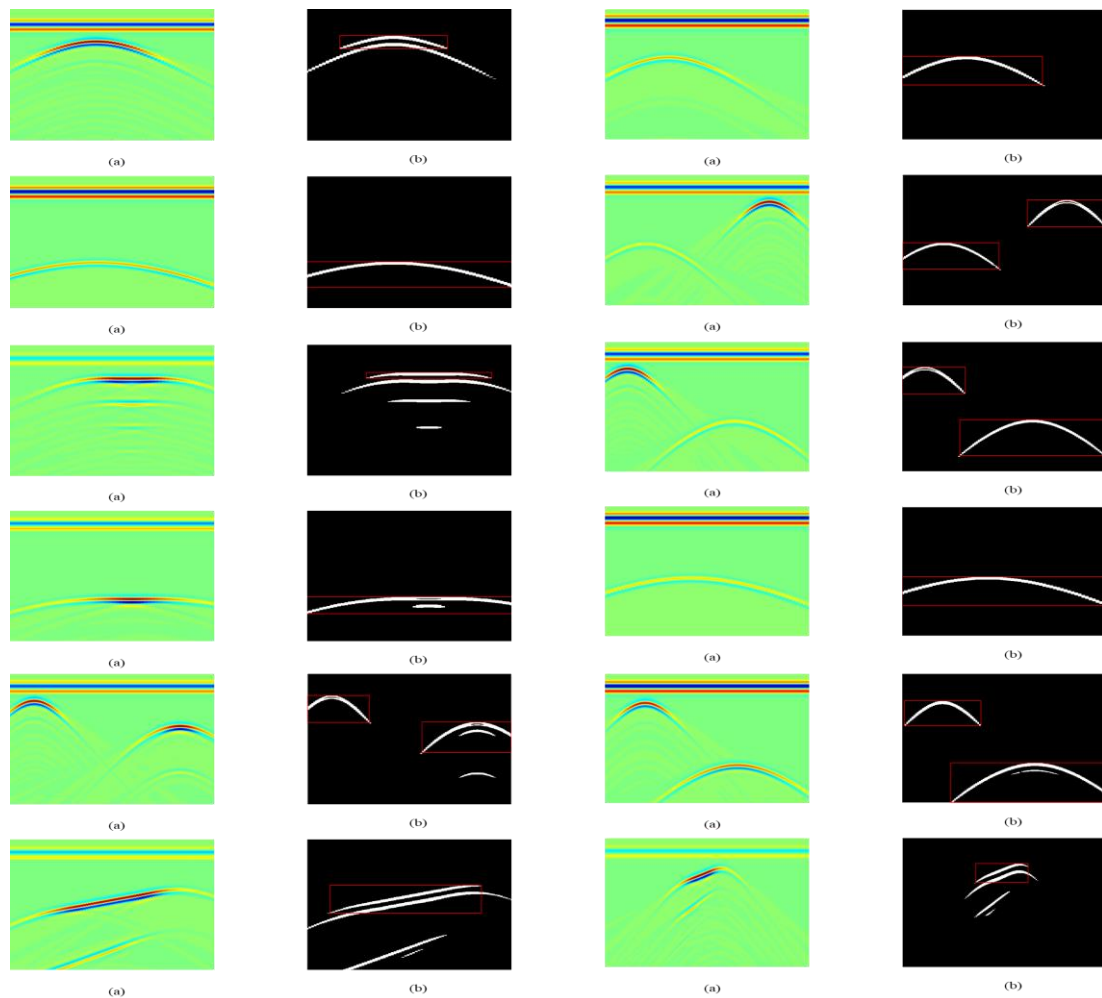


Figure 5. a) Original images, b) Segmented images using proposed algorithm

The proposed algorithm performance changes between 0.3794s and 2.232s. The average processing time is 1.4066s. Table 1 shows that processing time of proposed algorithm for each GPR B scan images.

**Table 1. Proposed algorithm performance**

Image ID	Performance
1	1.5009
2	0.7490
3	1.0557
4	0.7583
5	0.9374
6	0.9883
7	1.2123
8	2.2320
9	0.8567
10	0.9547
11	0.3794
12	1.5009

The obtained results are compared with results of other studies in the literature. Comparison results can be seen in Table 2.

**Table 2. Comparison of performance**

Study	Performance
	8s
Singh and Nene, 2013 [14]	43.8s – 255.6s
Chomdee et. al., 2014 [15]	
Proposed Method	0.3794s-2.2320s

## Conclusion

In this paper, fast and effective fully automated GPR B scan image segmentation method is presented. The proposed method is basically based on thresholding and hough transform. The general purpose is to segment the hyperbolas by eliminating background noise and ground plane. Thus, it is easy to detect buried objects location. It is performed in 8 different GPR B scan images. Hyperbolas of segmented images is quite successful. Finally, estimated buried object regions is drawn. Also, the process time is between 1.2342s-2.2320s. Compared to other proposed algorithms it works pretty fast. So, it can be under consideration in real time GPR applications. In the future, segmented GPR images which are obtained from proposed method can be used to detect buried object such as mines and pipe lines.

## References

- Levent Seyfi, Ercan Yıldız, A simulator based on energy efficient GPR algorithm modified for the scanning of all types of regions, Turk J Elec Eng & Comp Sci, Vol. 20 (3), 381-389, **2012**. DOI: 10.3906/elk-1011-955
- L. Capineri, P. Grande, and J. A. G. Temple, Advanced image-processing technique for real-time interpretation of ground-penetrating radar images, Int. J. Imaging Syst. Technol., vol. 9, no. 1, pp. 51–59, 1998.
- H. Brunzell, “Detection of shallowly buried objects using impulse radar,” IEEE Trans. Geosci. Remote Sens., vol. 37, no. 2, pp. 875–886, Mar. 1999.

- S. Delbò, P. Gamba, and D. Roccatò, "A fuzzy Shell clustering approach to recognize hyperbolic signatures in subsurface radar images," *IEEE Trans. Geosci. Remote Sens.*, vol. 38, no. 3, pp. 1447–1451, May 2000.
- P. Gamba and S. Lossani, "Neural detection of pipe signatures in ground penetrating radar images," *IEEE Trans. Geosci. Remote Sens.*, vol. 38, no. 2, pp. 790–797, Mar. 2000.
- W. Al-Nuaimy, Y. Huang, M. Nakhkash, M. T. C. Fang, V. T. Nguyen, and A. Eriksen, "Automatic detection of buried utilities and solid objects with GPR using neural networks and pattern recognition," *J. Appl. Geophys.*, vol. 43, no. 2–4, pp. 157–165, Mar. 2000.
- H. S. Youn and C. C. Chen, "Automatic GPR target detection and clutter reduction using neural network," in *Proc. 9th Int. Conf. Ground Penetrating Radar*, Santa Barbara, CA, 2002, vol. 4758, pp. 579–582.
- M. Rossini, "Detecting objects hidden in the subsoil by a mathematical method," *Comput. Math. Appl.*, vol. 45, no. 1, pp. 299–307, Jan. 2003.
- S. Shihab, W. Al-Nuaimy, and Y. Huang, "A comparison of segmentation techniques for target extraction in ground penetrating radar data," in *Proc. 2nd Int. Workshop Advanced GPR*, Delft, The Netherlands, 2003, pp. 95–100.
- P. Gamba and V. Belotti, "Two fast buried pipe detection schemes in ground penetrating radar images," *Int. J. Remote Sens.*, vol. 24, no. 12, pp. 2467–2484, Jan. 2003.
- P. Falorni, L. Capineri, L. Masotti, and G. Pinelli, "3-D radar imaging of buried utilities by features estimation of hyperbolic diffraction patterns in radar scans," in *Proc. 10th Int. Conf. Ground Penetrating Radar*, Delft, The Netherlands, 2004, vol. 1, pp. 403–406.
- A. Dell'Acqua, A. Sarti, S. Tubaro, and L. Zanzi, "Detection of linear objects in GPR data," *Signal Process.*, vol. 84, no. 4, pp. 785–799, Apr. 2004.
- L. Ting-Jun and Z. Zheng-Ou, "Fast extraction of hyperbolic signatures in GPR," in *Proc. ICMMT*, 2007, pp. 1–3.
- N. P. Singh and M. J. Nene, "Buried object detection and analysis of GPR images: Using neural network and curve fitting," *2013 Annual International Conference on Emerging Research Areas and 2013 International Conference on Microelectronics, Communications and Renewable Energy*, 2013.
- P. Chomdee, A. Boonpoonga and A. Prayote "Fast and Efficient Detection of Buried Object for GPR Image" *The 20th Asia-Pacific Conference on Communication*, pp. 350- 355, 2014.

---

### Author Information

---

**Gozde Altin**

Electronical and Telecommunication Engineering  
Kocaeli University (Kocaeli, Turkey)  
HAVELSAN (Istanbul, Turkey)  
Contact E-mail: [gozde.altin06@gmail.com](mailto:gozde.altin06@gmail.com)

**Arif Dolma**

Electronical and Telecommunication Engineering  
Kocaeli University (Kocaeli, Turkey)

---